Pergamon

Geochimica et Cosmochimica Acta, Vol. 66, No. 15, pp. 2791–2800, 2002

0016-7037/02 $22.00 + .00

PII S0016-7037(02)00872-4

Copper solubility in a basaltic melt and sulfide liquid/silicate melt partition coefficients of Cu and Fe

EDWARD M. RIPLEY,* JAMES G. BROPHY and CHUSI LI
Department of Geological Sciences, Indiana University, Bloomington, IN 47405, USA

(*Received June* 29, 2001; *accepted in revised form February* 22, 2002)

Abstract—The solubility of copper in a sulfur-saturated basaltic melt has been determined at 1245°C as a function of fO_2 and fS_2. Copper solubilities at log fO_2 values between −8 and −11 fall into two distinct populations as a function of fS_2. At log fS_2 values < -1.65, sulfide liquid that coexists with the basaltic glass quenches to sulfur-poor bornite solid solution. At log fS_2 values in excess of −1.65, the sulfide liquid quenches to a complex intergrowth of sulfur-rich bornite and intermediate solid solution. Copper solubilities in the low-fS_2 population range from 594 to 1550 ppm, whereas those in the high-fS_2 population range from 80 to 768 ppm. Sulfide liquid/silicate liquid partition coefficients (D) for Cu and Fe range from 480 to 1303 and 0.7 to 13.6, respectively. Metal-sulfur complexing in the silicate liquid is shown to be insignificant relative to metal-oxide complexing for Fe but permissible for Cu at high fS_2 values. On log D_{Fe} (sulfide-silicate) and log D_{Cu} (sulfide-silicate) vs. ½(log fS_2 − log fO_2) diagrams, both fS_2 populations show distinct but parallel trends. The observation of two D values for any fS_2/fO_2 ratio indicates nonideal mixing of species involved in the exchange reaction. The two distinct trends observed for both Cu and Fe are thought to be due to variations in activity coefficient ratios (e.g., $\gamma_{FeO}/\gamma_{FeS}$ and $\gamma_{CuO_{0.5}}/\gamma_{CuS_{0.5}}$). Results of the experiments suggest that accurate assessments of fS_2/fO_2 ratios are required for the successful numerical modeling of processes such as the partial melting of sulfide-bearing mantle and the crystallization of sulfide-bearing magmas, as well as the interpretation of sulfide mineralogical zoning. In addition, the experiments provide evidence for oxide or oxy-sulfide complexing for Cu in silicate magmas and suggest that the introduction of externally derived sulfur to mafic magma may be an important process for the formation of Cu-rich disseminated magmatic sulfide ore deposits.

1. INTRODUCTION

Knowledge of the solubility of metals in mafic magmas and the distribution of metals between silicate and sulfide minerals and liquids is required for accurate modeling of processes that lead to ore genesis. There have been several studies of partitioning behavior of platinum group elements (PGE) and siderophile elements (see Barnes and Maier, 1999, for a summary) as well as several studies that document the solubility of metals in silicate melts of various compositions (e.g., Capobianco and Amelin, 1994; Dingwell et al., 1994; Holzheid et al., 1994; Ripley and Brophy, 1995; Holzheid and Lodders, 2001). These studies have shown the importance of variables such as *T*, fO_2/fS_2, and melt composition in controlling metal solubility in silicate melts and metal distribution between metal or sulfide and silicate melt. Only a few studies have considered the partitioning behavior of Cu between sulfide and silicate liquids (e.g., Rajamani and Naldrett, 1978; Francis, 1990; Peach et al., 1990; Gaetani and Grove, 1997; Holzheid and Lodders, 2001), although it is of major significance for magmatic ore genesis. The work by Gaetani and Grove (1997) was done using a synthetic komatiite and a composition representative of a barred olivine chondrule. They showed the strong control of fS_2/fO_2 ratios on the distribution of Cu between sulfide and silicate melt, and olivine. The recent work by Holzheid and Lodders (2001) was done in alloy-saturated anorthite-diopside and basaltic melts. Results of both Gaetani and Grove's (1997) and Holzheid and Lodders's (2001) studies have been applied to core formation in the Earth and on Mars.

Although many magmatic Cu-Ni-Co deposits are characterized by Cu/Ni ratios of <1 (e.g., Naldrett, 1989), some deposits are characterized by much higher Cu/Ni ratios. Cu-rich deposits are most commonly those associated with continental flood basalt provinces, such as the Midcontinent Rift System, the Permian basalts of the Noril'sk area (Siberia), and the Central Flood Basalt Province of Southern Africa. An important example is the mineralization found in the lower portions of troctolitic rocks of the Duluth Complex (Minnesota, USA). Ratios of Cu/Ni in the mineralized rocks range from 5:1 to 3:1 (Ripley and Alawi, 1986). Elevated ratios of this type are often attributed to the separation of a Cu-enriched liquid during fractional crystallization of a more Fe-rich sulfide liquid (e.g., Craig and Kullerud, 1969; Fleet and Pan, 1994; Li et al., 1996). For example, massive Cu-rich vein-style ores at Sudbury (Li et al., 1992) and the Duluth Complex (Ripley and Alawi, 1986) are thought to have been produced as a result of the segregation of a Cu-enriched liquid that separated from a sulfide melt that was undergoing fractional crystallization. The dispersion of such a Cu-enriched liquid into a silicate magma to explain Cu-rich disseminated sulfide mineralization is not easily envisioned. The disseminated sulfides present in the troctolitic to gabbroic rocks of the Duluth Complex appear to be the result of interstitial crystallization of a Cu-rich sulfide liquid that was an integral component of the silicate magma. Not only are well-constrained sulfide liquid–silicate liquid distribution coefficients necessary to better understand these Cu-rich ores, but data on the solubility of Cu in mafic magmas and mechanisms

* Author to whom correspondence should be addressed (ripley@indiana.edu).

Table 1. Electron microprobe analysis of starting composition (wt.%) for Cu solubility and partition coefficient experiments. This composition was doped with either 2 or 10 wt.% CuO.

SiO_2	49.74
TiO_2	0.70
Al_2O_3	17.48
FeO	9.54
MnO	0.03
MgO	9.26
CaO	11.17
Na_2O	2.02
K_2O	0.14
P_2O_5	0.05
	100.13

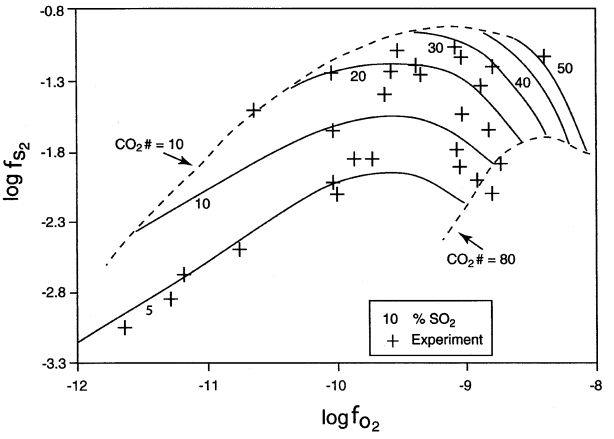

Fig. 1. Log fO_2 − log fS_2 plot showing contours for percentage SO_2 in the furnace gas mixture, CO_2 # (=[CO_2/(CO_2 + H_2)] × 100), and individual experiments. Most experiments were performed at CO_2 #s between 10 and 80.

of dissolution are needed to evaluate the potential roles of externally introduced sulfur and copper in ore genesis. Isotopic evidence (e.g., Ripley, 1999) strongly indicates that externally derived sulfur is an important ingredient for the formation of many large magmatic sulfide deposits. For metals such as Ni that may be oxide bonded and, in the absence of sulfide, reside in minerals such as olivine, the potential importance of externally derived sulfur for ore genesis is clear. However, Cu is thought to be held primarily as a sulfide in the mantle (e.g., Lorand, 1989), and the potential importance of externally derived sulfur for Cu-rich mineralization is less clear unless Cu may dissolve in a basaltic partial melt as an oxide, another S-free complex, or an oxy-sulfide complex.

To better constrain the controls on Cu solubility and sulfide liquid/silicate liquid partitioning behavior in tholeiitic melts, we initiated a series of experiments at variable fS_2/fO_2 conditions. Results of the experiments are used in conjunction with the earlier work by Ripley and Brophy (1995) on Cu solubility in S-free mafic melts to evaluate the controls of Cu solubility in mafic magmas and the potential importance of melt–country rock interaction in the genesis of Cu-rich sulfide mineralization. Parallel sets of solubility and partitioning experiments are in progress for Ni-bearing but Cu-free tholeiitic melts. Experiments containing both Cu and Ni will then be initiated to more closely approximate conditions of Cu-Ni sulfide ore deposition.

2. EXPERIMENTAL METHODS

The starting composition was a synthetic, high-Al, olivine tholeiite prepared with a mixture of SPEX ultrapure oxides and carbonates that were ground to <240 mesh. Several aliquots of this initial powder were fused at 1245°C on a platinum loop for 6 h at an fO_2 value equivalent to QFM ($10^{-7.8}$). The fused synthetic basalt (Table 1) was then ground to a fine powder and mixed with CuO to yield starting compositions with either 10 or 2 wt.% CuO (~8 or 1.6 wt.% Cu). This mixture was itself ground to <240 mesh to create the final starting material.

Thirty to 40 mg of the starting powder were placed into 3- to 4-mm diameter holes drilled into crystals of San Carlos olivine. The olivine crucibles are essentially inert and highly resistant to potential corrosion resulting from the sulfur-rich atmosphere. Individual crucibles were placed in quartz glass jackets and suspended by Pt support wires in a 1-atm Deltec furnace. Temperature was monitored using a Pt-$Pt_{90}Rh_{10}$ thermocouple calibrated against the melting point of Au. Gas fugacities were controlled by flowing mixtures of CO_2, H_2, and SO_2 over the sample. Gases entered the furnace through a water-cooled, O-ring-sealed stainless steel fitting at the top of a 2.5-cm inner diameter ceramic muffle tube. Flow rates ranged from 0.3 to 3.8 cm^3/s. Experiments were run for 24 to 48 h and quenched by cutting the Pt support wires and dropping the charge into a flask of chilled H_2O. Gas fugacities were computed using a free energy minimization technique (Outokumpu Research HSC Chemistry Version 4).

Experiments were conducted at 1245°C at a series of log fO_2 and log fS_2 conditions from ~wustite-magnetite (WM, $10^{-8.0}$) to ~3 log units below WM (Fig. 1). Chemical analyses were made using a CAMECA SX-50 four-spectrometer electron microprobe. Glass was analyzed using a 5-μm beam, 15-kV accelerating voltage, 20-nA beam current, and 20-s count time. Standards included a series of basaltic glasses. Copper and S in the silicate glasses were determined using a beam current of 100 nA and a counting time of 100 s. Detection limits were 80 ppm for Cu and 60 to 70 ppm for S. Sulfides were analyzed using a 20-nA beam current, 20-s count time, and a beam size of 10 to 20 μm. At least 10 analyses were made for each sample, with multiple broad-beam analyses averaged to determine the liquid composition for the samples with quench intergrowths. This method was also checked by analysis of 2-μm spots and liquid compositions calculated using image analysis and mass balance. Results of the two methods agree within 10%. Our primary standard was a synthetic $CuFeS_2$, with several secondary sulfide standards used for check purposes. The average deviation for the compositions of the check standards was <2% (relative). Oxygen in the quenched sulfide melts was analyzed by electron microprobe analysis using a PC2 crystal with a detection limit of ~0.1 wt.%.

Equilibration in the experimental charges was demonstrated only by the reproducibility of data collected from runs at the same conditions. Previous studies in the S-free system (Ripley and Brophy, 1995) demonstrated that equilibration was achieved within 24 h at 1245°C. Duplicate samples in this study run for 24, 48, and 72 h produced solubility data and distribution coefficients that varied by <10%.

3. RESULTS

Run products generally consisted of a large sulfide bead (0.7 to 1.0 mm diameter) at the top of the produced silicate glass (Fig. 2). The silicate glass contained <3% olivine crystals. Quenched sulfide liquid shows a broad compositional range that spans the central portion of the Cu-Fe-S system (Fig. 3). Two textural variations are recognized: one is homogeneous, with only rare, exsolved, native Cu along fractures, whereas the other is a more typical quench intergrowth (Fig. 4). In general, the homogeneous varieties are Cu rich and represent compositions in the bornite solid solution field. The coarser intergrowths are more S rich, with most bulk compositions represented by bornite solid solution plus intermediate solid solution

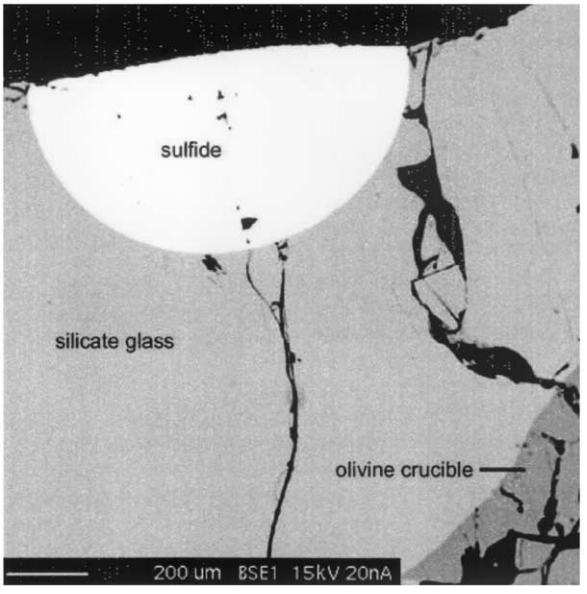

Fig. 2. Back-scattered electron image of a sulfide bead located at the top of a basaltic glass.

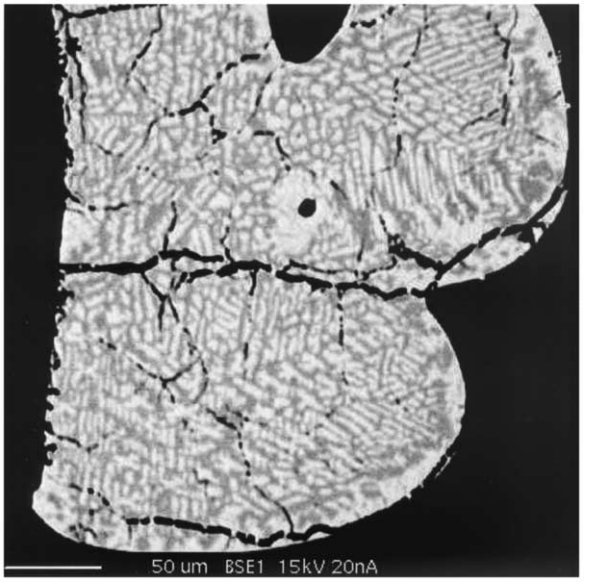

Fig. 4. Back-scattered electron image of a typical texture of sulfide liquid. Sample 43: 2% CuO. The light areas are bornite ss and the darker areas are iss.

or bornite solid solution plus intermediate solid solution plus pyrrhotite solid solution (on the basis of the 600°C phase diagram of Cabri, 1973). One sample was very rich in Fe, with a bulk composition represented by a mixture of bornite plus troilite plus iron. The more S-rich textural varieties are produced under higher log fS_2 conditions (typically >1.65) than the compositionally homogeneous samples (log $fS_2 < -1.65$). In Figures 5 to 10, our data are generally divisible into two populations that we refer to as either "high-fS_2" or "low-fS_2." These groups can also be distinguished on the basis of sulfide mineralogy or sulfide melt chemical composition.

Results of Cu solubility experiments are illustrated in Figures 5 to 10, and given in Table 2. In a plot of log fO_2 vs. Cu concentration in the silicate melt, the data define two reasonably linear populations (Fig. 5). Copper solubility ranges from 594 to 1550 ppm in the low-fS_2 runs and from 80 to 768 ppm in the high-fS_2 runs. At log fO_2 values > -11, the Cu solubility

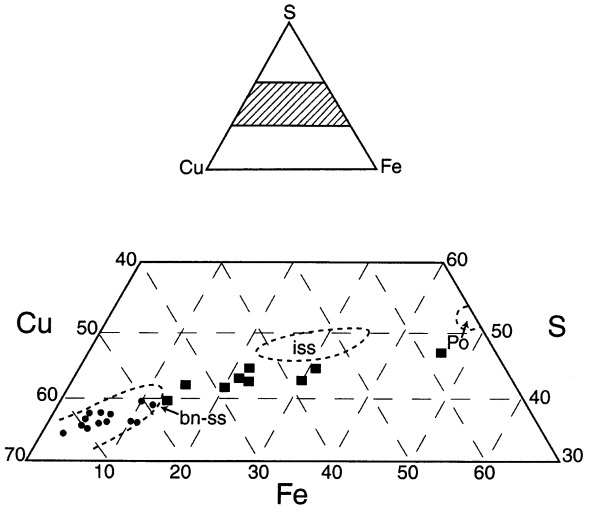

Fig. 3. Sulfide run products plotted in the Cu-Fe-S system (atomic). Bornite solid solution (ss) and intermediate solid solution (iss) fields are from the 600°C data of Cabri (1973).

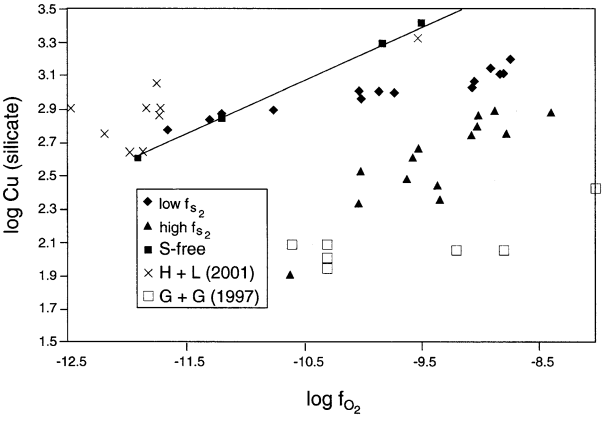

Fig. 5. Cu solubility data vs. log fO_2. Data for the S-free system are from Ripley and Brophy (1995) and were collected using a starting composition similar to that in this study. The high-fS_2 experiments were run at log $fS_2 > -1.65$ and generally produced a quenched sulfide liquid represented by bornite solid solution plus intermediate solid solution. The low-fS_2 experiments were conducted at log $fS_2 < -1.65$ and produced a quenched sulfide liquid represented by bornite solid solution. Data from Gaetani and Grove (1997) (G + G) are for komatiitic compositions and were collected at a temperature of 1350°C and log fS_2 values in excess of -2. Data from Holzheid and Lodders (2001) (H + L) are for MgO-rich basaltic compositions and were collected at a temperature of 1300°C and log fS_2 values < -2.5. It is clear that significantly lower Cu solubilities are obtained in high-fS_2 systems (our high-fS_2 runs and Gaetani and Grove's [1997] data) relative to low-fS_2 systems (our low-fS_2 runs and Holzheid and Lodders's [2001] data).

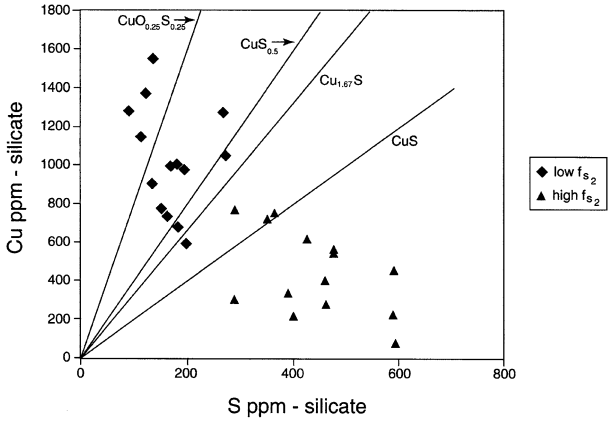

Fig. 6. S vs. Cu in the silicate glass. Note the restricted range in S content and large range in Cu concentration in the low-fS_2 population relative to those of the high-fS_2 population. Samples from the high-fS_2 population contain sufficient S in the silicate glass to balance Cu in the form of dissolved Cu-S complexes (various stoichiometries shown). The low-S, high-Cu samples from the low-fS_2 population contain insufficient S to balance Cu as a sulfide-only complex.

values are lower than those determined in the S-free system by Ripley and Brophy (1995), whereas at log fO_2 values between −11 and −11.5, the solubility values of the low-fS_2 population are within error of those in the S-free system. Data from Gaetani and Grove (1997) and Holzheid and Lodders (2001) are also shown in Figure 5. Sulfur solubility ranges from 288 to 592 ppm in the high-fS_2 runs and from 90 to 271 ppm in the low-fS_2 runs, with no discernable trends as a function of fO_2. Our high-fS_2 runs show S solubilities that are very similar to values reported by Haughton et al. (1974), whereas the S values in the low-fS_2 runs are considerably lower. When both fS_2 populations are considered together, the Cu content of the silicate glass is seen to increase as S content decreases (Fig. 6). The low-fS_2 population in particular shows very little variation in S content of the silicate glass with changing Cu concentration. Our charges were not doped with Fe; hence, the final glasses have a restricted range of FeO values between 8.52 and 4.69 wt.% (Table 3). Total Fe values have been corrected for Fe^{3+} contribution (<16.7‰) using the MELTS program of Ghiorso and Sack (1995).

Sulfide melt–silicate melt D values (Nernst distribution coefficient; concentration of metal in sulfide/concentration of metal in silicate) for both Cu and Fe also define two populations in log fO_2 − log D space as a function of log fS_2. Iron D (sulfide-silicate) values range from 2.7 to 13.6 in the high-fS_2 runs and from 0.7 to 2.8 in the low-fS_2 runs (Fig. 7a). Copper D (sulfide-silicate) values fall between 755 and 1303 in the high-fS_2 runs and between 480 to 969 in the low-fS_2 runs (Fig. 7b). The D values essentially encompass those determined by Rajamani and Naldrett (1978) in ultramafic melts, Peach and Mathez (1993) in basaltic melts, and Gaetani and Grove (1997) in komatiitic melts. Values of D_{Fe} (sulfide-silicate) are strongly related to the composition of the sulfide liquid (Figs. 8a and 8c). Values of D_{Cu} also vary with the composition of the sulfide liquid, but our data exhibit much more variability than for Fe (Fig. 8d). Values of D_{Cu} (sulfide-silicate) also vary with metal/sulfur ratio of the sulfide liquid when both fS_2 populations are

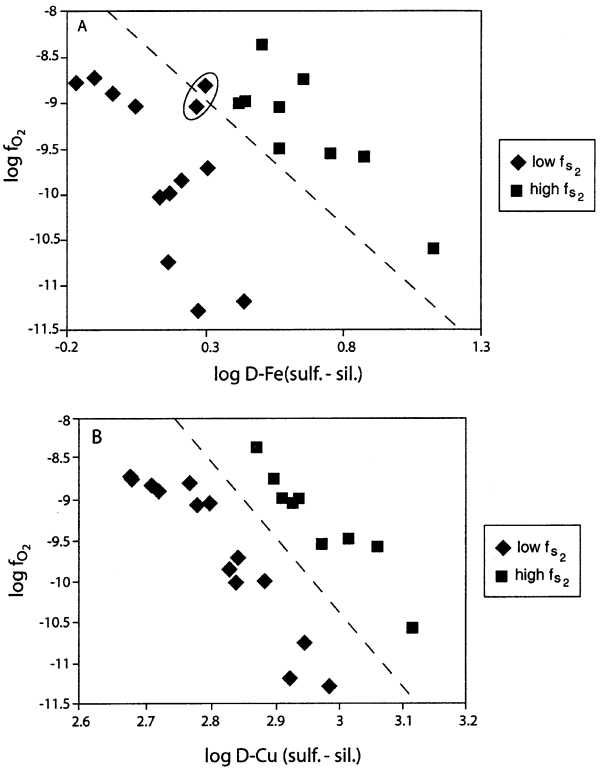

Fig. 7. (A) Log D-Fe (sulfide-silicate) vs. log fO_2, showing the clear separation between high- and low-fS_2 populations. The two circled samples contain quenched sulfide liquids that are the most Fe and S rich of those in the field of bornite solid solution and were produced at log fS_2 values of −1.65 and −1.79. With respect to Fe, their characteristics are often intermediate to those of the low- and high-fS_2 populations. (B) Log D-Cu (sulfide-silicate) vs. log fO_2.

considered together but show no systematic trends when the populations are considered independently (Fig. 8b).

In the low-fS_2 experiments, which were processed with both 2 and 10 wt.% CuO, there is no difference between D values observed at various fS_2/fO_2 ratios. In other words, the equilibrium between silicate and sulfide liquids was unaffected; only the relative size of the sulfide bead varied (larger in runs with 10% CuO). The size of the sulfide bead was larger in the high-fS_2 runs than in the low-fS_2 runs; this is consistent with the more chalcophile behavior of Fe with increasing fS_2. Because Fe became more chalcophile at the higher fS_2 conditions, the atomic percentage of Cu in the sulfide decreased, even though D_{Cu} (sulfide-silicate) values increased (Fig. 8d). It should be recalled that the computed Nernst partition coefficients (D values) are not equilibrium constants (see below), and intrinsic stoichiometries may vary.

4. DISCUSSION

The solution of chalcophile elements in mafic melts is generally considered in terms of exchange reactions of the form

$$FeO_{silicate} + \tfrac{1}{2}\, S_2 = FeS_{sulfide} + \tfrac{1}{2}\, O_2 \qquad (1)$$

or

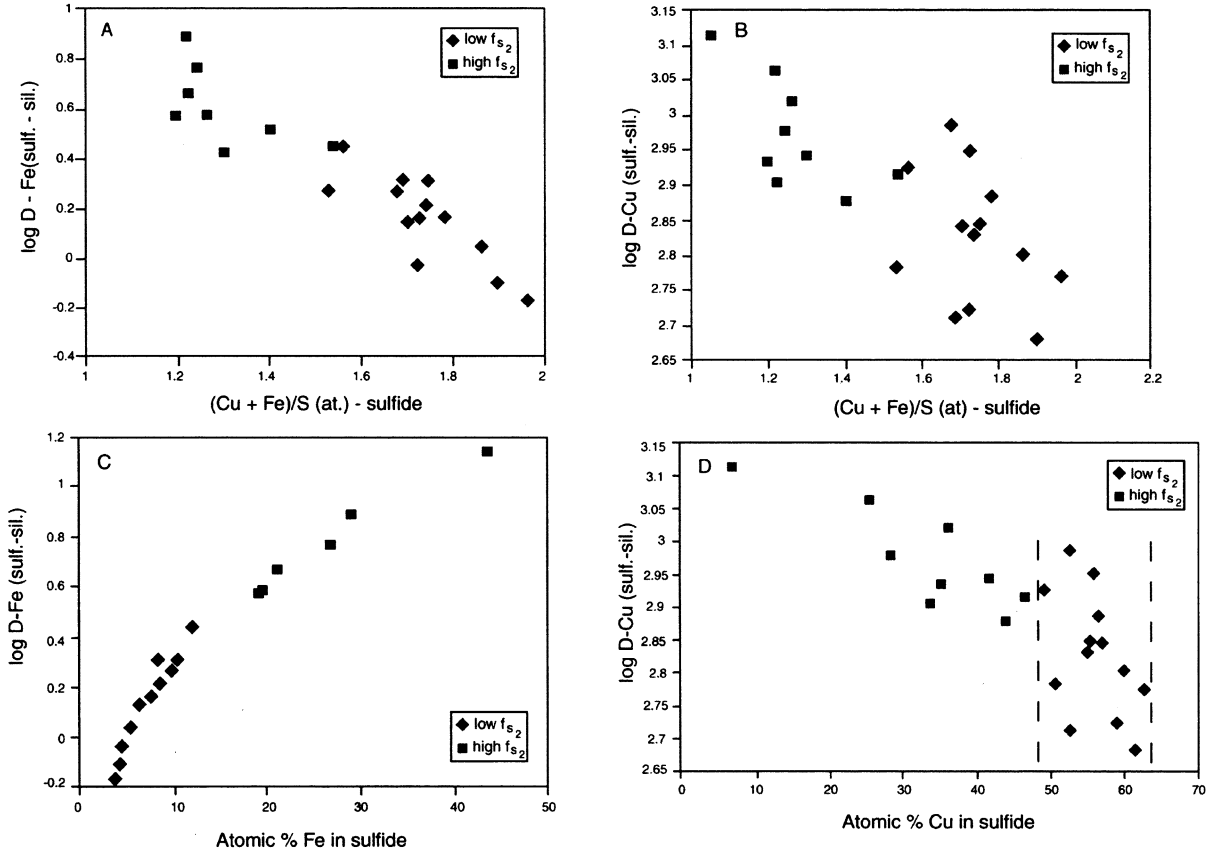

Fig. 8. (A) Variation in log *D*-Fe (sulfide-silicate) vs. Cu + Fe/sulfur ratio in the sulfide liquid. (B) Variation in log *D*-Cu (sulfide-silicate) vs. Cu + Fe/sulfur ratio in the sulfide liquid. When both populations are considered together, a general negative covariation is apparent. When evaluated independently, there is no correlation between metal/sulfur ratio and log *D*-Cu (sulfide-silicate) in the low-fS_2 samples. (C) Positive covariation between log *D*-Fe (sulfide-silicate) and atomic percentage Fe in the sulfide liquid. (D) Overall negative covariation between log *D*-Cu (sulfide-silicate) and atomic percentage Cu in the sulfide liquid. As with the metal/sulfur ratio vs. log *D*, there is no correlation between log *D*-Cu and atomic percentage Cu in the sulfide for samples from the low-fS_2 population.

$$CuO_{0.5(silicate)} + \tfrac{1}{4}\, S_2 = CuS_{0.5(sulfide)} + \tfrac{1}{4}\, O_2. \quad (2)$$

At the log fO_2 values of this study, the ratio of Fe^{3+}/Fe^{2+} in the silicate melt is $< \sim 0.16$. Hence, reaction 1 is considered to be appropriate for Fe. Ripley and Brophy (1995) have shown that in the sulfur-free system for a starting composition similar to that employed in this study, the dominant valence state of Cu is Cu^{+} (>75%) in the form of $CuO_{0.5}$. The equilibrium constant for reactions such as 1 and 2 may be written as

$$K = \frac{(a_{MeS_x})(fO_2)^{x/2}}{(a_{MeO_x})(fS_2)^{x/2}}, \quad (3)$$

where x is the number of anion atoms. By rearranging,

$$\log D(\text{molar}) = (x)\ \tfrac{1}{2}\ (\log fS_2 - \log fO_2) + \log K + \log\frac{\gamma MeO_x}{\gamma MeS_x}, \quad (4)$$

Peach and Mathez (1993) and Gaetani and Grove (1997) highlighted the fact that if activity coefficient ratios are constant, then a plot of log *D* (either molar or converted to concentration

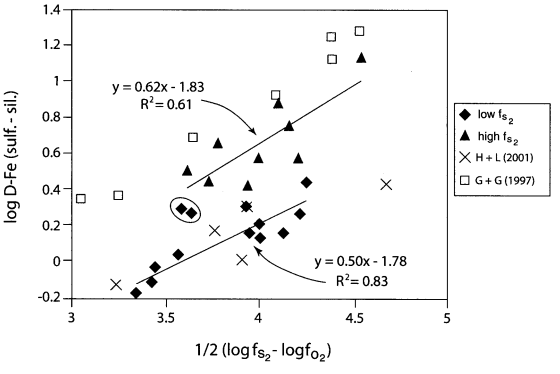

Fig. 9. Log *D*-Fe (sulfide-silicate) vs. ½(log fS_2 − log fO_2). The two circled samples contain the most Fe- and S-rich bornite solution in the low-fS_2 population as described in Figure 7. These samples have been excluded from the regression for the low-fS_2 population. The data from Gaetani and Grove (1997) (G + G) and Holzheid and Lodders (2001) (H + L), described in Figure 5, are consistent with the existence of two distinct trends in *D*-Fe values for samples produced under high-fS_2 conditions and that contain S-rich sulfide liquids (e.g., intermediate solid solution) and under low-fS_2 conditions and that contain S-poor sulfide liquids (e.g., bornite solid solution).

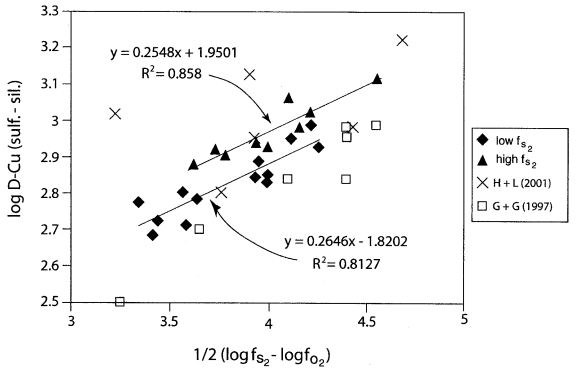

Fig. 10. Log D-Cu (sulfide-silicate) vs. ½(log fS_2 − log fO_2). The distinction between high-fS_2 and low-fS_2 populations is not as distinct as for Fe, but still discernable. G + G = Gaetani and Grove (1997); H + L = Holzheid and Lodders (2001).

of metal in the sulfide/concentration of metal in the silicate) vs. the fS_2/fO_2 ratio should yield a straight-line relationship. In a plot of log D vs. ½(log fS_2 − log fO_2) for divalent metals such as Fe, the expected slope is 1, whereas for monovalent Cu, the predicted slope is 0.5. For both Fe and Cu, linear relationships between log D and ½(log fS_2 − log fO_2) are observed (Figs. 9 and 10). However, for Fe, there are two essentially parallel, linear trends that correspond to the two fS_2 populations referred to above, as well as to the composition of the quenched sulfide liquid. The experiments of Gaetani and Grove (1997) and Holzheid and Lodders (2001) were done at higher temperatures than ours, but their data confirm the two populations observed for Fe. Data from Gaetani and Grove (1997) were collected at relatively high log fS_2 conditions (>-2), at which the quenched sulfide liquid was S rich (30.0 to 36.8 wt.% S). Their data plot slightly above our high-fS_2 results in log D − ½(log fS_2 − log fO_2) space. Holzheid and Lodders's (2001) experiments were performed at much lower log fS_2 conditions (<-2.5 and most <-4), at which the quenched sulfide liquid was characterized by low S (20.1 to 22.9 wt.% S in their Fe-bearing system) and high Cu. The sulfide liquid was very similar in composition to the bornite solid solution produced in our low-fS_2 experiments, and the D-Fe (sulfide-silicate) values fall within our low-fS_2 population in Figure 9.

For Cu, the distinction between low- and high-fS_2 populations is not as well defined, although the two populations remain discernable (Fig. 10). Our data parallel the trend observed by Gaetani and Grove (1997), although their data plot slightly below ours in log D-Cu (sulfide-silicate) − ½(log fS_2 − log fO_2) space. The data points computed from Holzheid and Lodders's (2001) experiments are scattered in Figure 10, with some points overlapping those of this study and three points showing much higher log D-Cu (sulfide-silicate) values. The experiments of Holzheid and Lodders (2001) were also saturated in native Cu or a Cu-rich alloy and for this reason may not be directly comparable with the data collected in this study.

For Fe, our data, uncorrected for Fe^{3+} contribution, yield slopes of ~0.70 and ~0.55 for the high- and low-fS_2 populations, respectively. However, D_{Fe} (sulfide-silicate) computed assuming only ferrous iron in the silicate melt must be corrected for the contribution of Fe^{3+} to the total Fe content, coupled with the involvement of O in the sulfide melt. We have corrected our values for Fe^{3+} contribution to the silicate total Fe content (see below) and have assigned O in the sulfide melt to Fe^{2+}. D values were computed using only sulfide-bonded Fe. The possible contribution of Fe^{3+} to the sulfide melt has not been evaluated. As the ratio of Fe^{3+}/Fe^{2+} in the silicate melt increases and the value of ½(log fS_2 − log fO_2) declines, D-Fe values would be expected to increase. This causes a shallowing of the slope predicted from reaction 1, where all Fe is divalent. However, because Fe^{3+} contributes <16.7% to the total Fe content of our runs, the slope modification is not large. Corrected slopes for the two populations of D_{Fe} (sulfide-silicate) values are 0.50 and 0.62 (±0.05, Fig. 9).

Holzheid and Lodders (2001) suggested that the presence of Cu^{2+} in the experiments of Ripley and Brophy (1995) may be related to alkali element reaction with iron, in combination with copper-iron redox reactions of the form

$$Cu^{+} + Fe^{3+} = Fe^{2+} + Cu^{2+}. \quad (5)$$

If Fe^{3+} combines with Na^{+} or K^{+} to form complexes such as $(FeNa)^{4+}$, the Fe^{3+}/Fe^{2+} ratio in the silicate melt may increase. This could also cause a shallowing of the slope observed in log D − ½(log fS_2 − log fO_2) plots, as described above. However, reactions such as 5 that may explain increases in Cu^{2+} abundance would also tend to counteract both increases in Fe^{3+} abundance and shallower than expected slopes in log D − ½(log fS_2 − log fO_2) space.

Gaetani and Grove (1997) discussed how the involvement of metal-sulfur species in the silicate melt can lead to a weaker observed dependency of D values on the fS_2/fO_2 ratio. However, because of the relatively low values of dissolved sulfur in the silicate melts, mass balance calculations indicate that this mechanism can impart a change in slope of <3% and is less effective than the Fe^{3+} contribution to total Fe in causing a shallowing of the log D − ½(log fS_2 − log fO_2) slope. The possibility of this mechanism for Cu is discussed more fully below. The distinct lines observed for the high-fS_2 and low-fS_2 populations in log D_{Fe} (sulfide-silicate) − ½(log fS_2 − log fO_2) space indicate nonideal mixing of species involved in the exchange reaction and hence variation in the ratios of

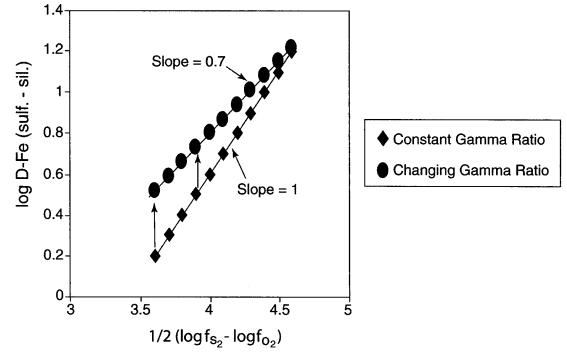

Fig. 11. Example change in slope produced from an increase in the ratio $\gamma_{FeO}/\gamma_{FeS}$ of 0.03 per 0.1 unit of ½(log fS_2 − log fO_2). Computed using log D = ½(log fS_2 − log fO_2) + log K + log $\gamma_{FeO}/\gamma_{FeS}$. The cumulative change in the activity coefficient ratio with fS_2/fO_2 ratio produces a slope < 1 in a log D − ½(log fS_2 − log fO_2) plot.

Table 2. Run conditions and experimental results.

Experiment number	Initial wt.% CuO	log fS_2	log fO_2	Fe silicate (wt.%)	Cu silicate (ppm)	S silicate (ppm)	O sulfide (wt.%)
12	10	–3.05	–11.65	4.66	594 (60)	199 (20)	sl
22	2	–2.85	–11.29	5.81	677 (51)	182 (30)	0.79 (.03)
29	10	–2.68	–11.19	4.96	733 (44)	163 (19)	0.19 (.04)
14	10	–2.50	–10.75	5.78	775 (76)	151 (24)	0.29 (.03)
21	2	–2.11	–8.79	6.19	1278 (120)	90 (25)	0.12 (.03)
20	2	–2.10	–10.00	6.19	902 (80)	134 (11)	0.12 (.03)
27	10	–2.02	–1.02	5.19	1003 (53)	180 (20)	0.51 (.04)
28	10	–2.01	–8.90	5.69	1369 (55)	121 (16)	0.12 (.04)
30	10	–1.91	–9.04	5.73	1144 (58)	112 (22)	0.12 (.03)
31	2	–1.89	–8.73	6.11	1550 (87)	136 (39)	0.12 (.03)
31	10	–1.86	–9.72	4.69	977 (100)	194 (23)	1.10 (.04)
23	2	–1.85	–9.85	5.97	998 (94)	170 (27)	0.24 (.04)
37	2	–1.79	–9.06	6.43	1050 (25)	271 (43)	0.14 (.03)
39	2	–1.65	–8.82	6.17	1268 (108)	267 (41)	0.21 (.04)
38	2	–1.54	–9.01	5.98	720 (78)	350 (59)	0.28 (.03)
40	2	–1.51	–10.62	3.64	80 (19)	592 (60)	3.03 (.03)
43	2	–1.40	–9.62	4.44	300 (40)	288 (53)	1.44 (.04)
30	2	–1.24	–9.57	5.34	401 (40)	460 (38)	2.11 (.04)
25	2	–1.21	–8.77	5.78	559 (59)	477 (50)	0.87 (.04)
26	2	–1.14	–9.02	6.34	619 (62)	426 (40)	2.29 (.04)
35	2	–1.14	–8.38	5.55	748 (40)	365 (28)	0.71 (.04)
28	2	–1.09	–9.52	6.07	457 (45)	589 (24)	1.42 (.04)
27	2	–1.07	–9.07	6.14	547 (73)	477 (23)	1.52 (.04)
42	2	–1.65	–10.01	5.84	333 (43)	391 (30)	sl
36	2	–1.20	–9.36	5.4	274 (30)	461 (40)	sl
37-b	2	–1.26	–9.34	6.31	225 (23)	587 (64)	sl
38-b	2	–1.34	–8.87	6.62	768 (71)	289 (29)	sl
39-b	2	–1.25	–10.03	6.14	213 (21)	401 (47)	sl

D-Fe values have been corrected for Fe^{3+} contribution to total silicate Fe and for Fe-O bonding in the sulfide. 1σ uncertainties on calculated *D*

Table 3. Electron microprobe analyses of silicate glass run products.

Run #	Initial wt.% CuO	P_2O_5	SiO_2	TiO_2	Al_2O_3	MgO
12	10	0.09 (.04)	52.70 (.88)	0.66 (.08)	17.94 (.28)	10.15 (.18)
22	2	0.08 (.04)	51.40 (.96)	0.66 (.09)	17.13 (.16)	8.86 (.06)
29	10	0.03 (.01)	51.98 (.30)	0.71 (.01)	17.99 (.34)	8.65 (.13)
14	10	0.12 (.06)	52.02 (.34)	0.70 (.05)	17.49 (.06)	10.17 (.27)
21	2	0.03 (.03)	51.72 (.18)	0.69 (.07)	17.35 (.67)	8.36 (.31)
20	2	0.03 (.03)	53.05 (.30)	0.69 (.03)	16.94 (.08)	9.81 (.10)
27	10	0.01 (.01)	50.48 (.59)	0.63 (.03)	16.88 (.14)	10.82 (.13)
28	10	0.12 (.04)	51.83 (.47)	0.72 (0.6)	17.03 (.25)	9.02 (.03)
30	10	0.12 (.02)	51.54 (.36)	0.62 (.28)	17.16 (.15)	9.05 (.06)
31	2	0.05 (.03)	51.86 (.75)	0.74 (.06)	18.11 (.19)	8.96 (.16)
31	10	0.10 (.01)	52.26 (.11)	0.59 (.09)	16.84 (.16)	8.82 (.15)
23	2	0.02 (.02)	52.26 (.11)	0.59 (.09)	16.84 (.16)	8.82 (.15)
37	2	0.05 (.07)	51.59 (.23)	0.62 (.02)	15.78 (.17)	11.10 (.10)
39	2	0.03 (.03)	51.64 (.35)	0.62 (.03)	16.27 (.18)	11.07 (.06)
38	2	0.03 (.03)	51.67 (.90)	0.62 (.02)	16.25 (.13)	11.18 (.06)
40	2	0.03 (.02)	54.40 (.24)	0.65 (.02)	16.90 (.10)	12.03 (.06)
43	2	0.03 (.03)	54.86 (.32)	0.61 (.02)	15.43 (.18)	11.92 (.14)
30	2	0.03 (.03)	52.47 (.23)	0.63 (.02)	16.63 (.27)	11.27 (.09)
25	2	0.05 (.03)	51.94 (.12)	0.67 (.03)	16.93 (.15)	10.65 (.08)
26	2	0.02 (.03)	51.49 (.05)	0.68 (.02)	16.70 (.08)	10.45 (.09)
35	2	0.02 (.01)	51.75 (.25)	0.65 (.02)	16.20 (.15)	11.15 (.10)
28	2	0.02 (.01)	51.76 (.22)	0.65 (.02)	16.86 (.18)	10.79 (.10)
27	2	0.02 (.01)	51.94 (.14)	0.69 (.03)	17.13 (.11)	10.54 (.08)
42	2	0.03 (.04)	52.02 (.51)	0.66 (.03)	16.67 (.17)	11.37 (.04)
36	2	0.02 (.03)	52.66 (.20)	0.65 (.02)	16.55 (.15)	11.30 (.11)
37-b	2	0.06 (.05)	52.27 (.23)	0.62 (.03)	16.26 (.17)	11.48 (.18)
38-b	2	0.01 (.01)	51.28 (.09)	0.63 (.02)	16.31 (.13)	10.74 (.06)
39-b	2	0.05 (.05)	52.38 (.35)	0.63 (.02)	16.63 (.18)	11.33 (.06)

$Fe_2O_3/(FeO + Fe_2O_3)$ calculated using MELTS (Ghiorso and Sack, 1995). Values in parentheses are 1σ uncertainties.

Table 2. (Continued)

S sulfide (wt.%)	Fe sulfide (wt.%)	Cu sulfide (wt.%)	*D*-Cu	*D*-Fe	(Cu + Fe)/ S atomic	Cu/Fe atomic	Fe/S atomic
sl	sl	sl	sl	sl	sl	sl	sl
22.51 (.13)	13.29 (.15)	63.41 (.27)	969	1.9	1.68	5.26	0.27
24.56 (.13)	13.85 (.11)	61.46 (.32)	843	2.8	1.56	4.07	0.31
22.48 (.12)	9.02 (.09)	68.30 (.34)	890	1.4	1.73	7.46	0.20
20.36 (.12)	2.16 (.04)	77.48 (.36)	592	0.7	1.96	17.65	0.10
22.10 (.12)	8.58 (.08)	69.32 (.34)	770	1.5	1.78	7.43	0.21
22.42 (.12)	8.50 (.08)	68.57 (.34)	698	1.4	1.70	8.92	0.17
22.67 (.15)	5.15 (.20)	72.50 (.22)	529	0.9	1.72	13.46	0.12
21.28 (.12)	6.14 (.07)	72.58 (.35)	636	1.1	1.86	11.09	0.15
20.94 (.12)	4.81 (.06)	74.24 (.36)	480	.08	1.90	14.79	0.12
22.21 (.12)	9.21 (.09)	67.48 (.33)	700	2.0	1.75	6.68	0.22
22.42 (.12)	9.91 (.09)	67.50 (.33)	682	1.6	1.74	6.50	0.23
24.97 (.13)	11.47 (.10)	63.56 (.31)	607	1.9	1.53	5.06	0.25
23.06 (.13)	11.89 (.11)	64.90 (.32)	512	2.0	1.68	5.08	0.27
24.81 (.14)	16.30 (.12)	58.66 (.31)	823	2.8	1.54	3.34	0.35
30.06 (.15)	57.86 (.28)	9.05 (.09)	1303	13.6	1.05	0.17	0.90
28.30 (.14)	37.06 (.22)	32.20 (.20)	1156	7.7	1.22	0.87	0.64
27.19 (.14)	36.06 (.19)	34.63 (.24)	951	5.8	1.24	1.05	0.60
28.91 (.15)	26.92 (.18)	43.29 (.24)	803	4.6	1.22	1.58	0.47
25.56 (.13)	23.29 (.15)	48.86 (.27)	877	2.7	1.30	2.79	0.34
26.05 (.14)	18.36 (.13)	54.81 (.29)	755	3.3	1.40	3.01	0.35
27.45 (.14)	26.19 (.12)	44.93 (.30)	1047	3.8	1.26	1.85	0.44
28.86 (.15)	26.50 (.22)	44.64 (.19)	859	3.7	1.20	1.84	0.42
sl	sl	sl	sl	sl	sl	sl	sl
sl	sl	sl	sl	sl	sl	sl	sl
sl	sl	sl	sl	sl	sl	sl	sl
sl	sl	sl	sl	sl	sl	sl	sl
sl	sl	sl	sl	sl	sl	sl	sl

values are less than 10%. sl = sulfide lost during sample preparation. Values in parentheses are 1σ uncertainties.

Table 3. (Continued)

CaO	MnO	FeO (total)	$\frac{Fe_2O_3}{FeO + Fe_2O_3}$	Na_2O	K_2O	Total
11.15 (.15)	0.03 (.02)	6.00 (.13)	0.032	1.66 (.04)	0.13 (.01)	100.50
10.75 (.09)	0.01 (.01)	7.47 (.03)	0.038	2.10 (.05)	0.13 (.01)	98.59
11.10 (.15)	0.01 (.02)	6.39 (.10)	0.040	1.88 (.02)	0.15 (.01)	98.87
10.86 (.07)	0.01 (.01)	7.44 (.30)	0.046	1.96 (.03)	0.13 (.01)	100.89
10.93 (.23)	0.01 (.01)	7.96 (.15)	0.108	1.97 (.02)	0.14 (.02)	99.15
9.95 (.09)	0.03 (.02)	7.97 (.15)	0.110	1.09 (.04)	0.11 (.01)	99.64
10.46 (.06)	0.02 (.01)	6.68 (.22)	0.062	1.90 (.05)	0.12 (.01)	98.01
11.32 (.08)	0.01 (.01)	7.32 (.10)	0.167	2.14 (.04)	0.14 (.01)	99.65
11.25 (.08)	0.02 (.01)	7.37 (.13)	0.099	2.13 (.04)	0.13 (.01)	99.36
11.56 (.14)	0.01 (.01)	6.04 (.16)	0.078	2.20 (.06)	0.14 (.01)	99.73
10.30 (.01)	0.01 (.01)	7.42 (.15)	0.069	1.95 (.01)	0.12 (.01)	98.33
10.30 (.01)	0.01 (.01)	7.42 (.15)	0.069	1.95 (.01)	0.12 (.01)	98.33
10.04 (.09)	0.04 (.01)	8.28 (.10)	0.087	1.35 (.02)	0.13 (.01)	98.98
10.31 (.08)	0.02 (.02)	7.94 (.15)	0.100	1.77 (.01)	0.15 (.01)	99.82
10.31 (.04)	0.02 (.02)	7.70 (.12)	0.092	1.70 (.02)	0.16 (.01)	99.63
10.57 (.10)	0.01 (.01)	4.69 (.21)	0.045	1.03 (.01)	0.11 (.01)	100.42
9.36 (.17)	0.01 (.01)	5.71 (.16)	0.058	1.28 (.01)	0.09 (.02)	99.30
10.41 (.08)	0.01 (.01)	6.92 (.12)	0.072	1.39 (.03)	0.13 (.02)	99.87
10.49 (.07)	0.02 (.01)	7.44 (.13)	0.103	1.62 (.04)	0.13 (.01)	99.94
10.44 (.09)	0.02 (.03)	8.11 (.14)	0.097	1.37 (.03)	0.10 (.01)	99.67
10.36 (.09)	0.01 (.01)	7.15 (.08)	0.120	1.65 (.02)	0.13 (.01)	99.07
10.42 (.07)	0.02 (.01)	7.81 (.25)	0.074	1.50 (.01)	0.12 (.02)	99.94
10.44 (.09)	0.02 (.02)	7.90 (.10)	0.090	1.46 (.03)	0.11 (.02)	100.24
10.46 (.12)	0.01 (.02)	7.51 (.18)	0.059	1.55 (.02)	0.15 (.01)	100.42
10.42 (.08)	0.02 (.01)	6.95 (.12)	0.079	1.45 (.02)	0.11 (.01)	100.13
10.24 (.10)	0.02 (.01)	8.12 (.10)	0.076	1.07 (.01)	0.08 (.01)	100.23
10.27 (.04)	0.02 (.02)	8.52 (.12)	0.098	1.70 (.01)	0.15 (.01)	99.63
10.28 (.08)	0.02 (.02)	7.91 (.15)	0.108	1.32 (.02)	0.13 (.01)	100.67

$\gamma_{FeS-sulfide\ melt}/\gamma_{FeO-silicate\ melt}$. Values of γ_{FeS} in the Fe-S (Nagamori et al., 1969) and Fe-Ni-S (Hsieh et al., 1987) systems have been found to decrease with increasing metal/sulfur ratio. This is consistent with our results for Fe, for which a strong positive relationship between log D_{Fe} (sulfide-silicate) and Fe/S (sulfide) ratio is observed. Because γ_{FeO} is likely to vary less than γ_{FeS} (e.g., Holzheid et al., 1997), log D_{Fe} (sulfide-silicate) values for higher metal/sulfur ratios (corresponding to low values of ½[log fS_2 − log fO_2]) will be greater than for lower metal/sulfur ratios. The overall effect in log D_{Fe} (sulfide-silicate) vs. ½(log fS_2 − log fO_2) space is a shallower slope relative to that predicted in the case of ideal mixing of the species in reaction 1. We therefore suggest that the two fS_2 populations observed for Fe in Fig. 9 result from large differences in γ_{FeS} and that the deviation within each population from the expected log D dependency on ½(log fS_2 − log fO_2) values results primarily from smaller changes in $\gamma_{FeO}/\gamma_{FeS}$ (Fig. 11).

For Cu, the observed slope of log D vs. ½(log fS_2 − log fO_2) is also less than that predicted from reaction 2. A feasible reason for this would be the complexing of Cu with S in the silicate melt. For example, in the case of 50% sulfide complexing, the following reaction may be written:

$$CuO_{0.25}S_{0.25(silicate)} + \tfrac{1}{8}\ S_2 = CuS_{0.5(sulfide)} + \tfrac{1}{8}\ O_2. \quad (6)$$

In log D − ½(log fS_2 − log fO_2) space, this reaction is represented by a slope of 0.25 if activity coefficient ratios are constant. As mentioned above, sulfidic dissolution of Fe is not a feasible mechanism to explain the shallower than expected slopes in log D_{Fe} (sulfide-silicate) − ½(log fS_2 − log fO_2) space because the concentration of dissolved S is too low to balance that of Fe. However, for Cu, only the most Cu-rich and S-poor samples from the low-fS_2 experiments are not consistent with reaction 6 (Fig. 6). Also illustrated in Figure 6 is the fact that the majority of the low-fS_2 runs are not compatible with Cu dissolution as a sulfidic species only. Holzheid and Lodders (2001) also found no evidence in their experiments for sulfidic dissolution of Cu in silicate liquids. Their experiments were performed at log fS_2 values < -2.5. Results from our high-fS_2 experiments indicate that Cu-S complexing in the silicate melt is permissible from a mass balance standpoint (Fig. 6). However, the observed dependency of D_{Cu} (sulfide-silicate) values on fS_2/fO_2 ratios suggests that some form of oxide or oxy-sulfide complexing is more appropriate.

Because of the absence of an Fe-rich, Cu-poor sulfide in any of the quench products except for run 40, a solution mechanism involving Cu-Fe complexing is reasonable. Reactions such as

$$Cu^{+}Fe^{2+}_{0.5}S_{0.75}O_{0.25} + \tfrac{1}{8}\ S_2 = CuFe_{0.5}S + \tfrac{1}{8}\ O_2 \quad (7)$$

are consistent with the observed slope, but Cu/Fe ratios in the sulfide of ~2:1 should result. Such ratios are found in only a few of our high-fS_2 runs (Table 2). At lower fS_2 conditions (lower ½[log fS_2 − log fO_2]), charge coupling may become important in the sulfide liquid. Vaughan and Burns (1972) showed using Mössbauer spectroscopy that Fe^{3+} and Cu^{+} are predominant in bornite. Reactions such as

$$Cu^{+}_{1.25}Fe^{2+}_{0.15}Fe^{3+}_{0.15}S_{0.75}O_{0.25} + \tfrac{1}{8}\ S_2 = Cu_{1.25}Fe_{0.30}S + \tfrac{1}{8}\ O_2 \quad (8)$$

would be consistent with the observed slope. Mass balance calculations also indicate that an appropriate concentration of Fe^{3+} would be available in the silicate melt; however, the Cu/Fe ratio in the sulfide is ~4:1 and in line with only a few of our low-fS_2 experiments (Table 2). Reactions similar to 4 and 5 also require molar Cu/S ratios < 1.67 in the silicate melt. Only in the basaltic glasses produced under high-fS_2 conditions is sulfur of sufficient concentration for such sulfur-bearing complexes to be of importance (Fig. 5).

The two populations observed for D_{Cu} (sulfide-silicate) values in Fig. 10, although not as distinct as those observed for Fe, clearly indicate nonideal mixing of species involved in the Cu exchange reaction. Different values of the activity coefficient ratio, $\gamma_{CuO_{0.5}}/\gamma_{CuS_{0.5}}$, can explain the presence of the two populations. As with Fe, very slight increases in the activity coefficient ratio with decreasing ½(log fS_2 − log fO_2) can result in slopes that are shallower than predicted in the case of ideal mixing. For Cu dissolution in the silicate melt, the presence of sulfide or oxy-sulfide complexes cannot be ruled out and may also contribute to the shallowness of the slopes observed in log D − ½(log fS_2 − log fO_2) space.

5. SUMMARY AND CONCLUSIONS

The solubility of copper in a sulfide-saturated olivine tholeiite liquid at 1245°C varies between 80 and 1550 ppm and is strongly related to the composition of the coexisting sulfide liquid, fO_2, and fS_2. At log fO_2 values between −8 and −11, copper solubility is less than that recorded under S-free conditions, but values are similar or greater at log $fO_2 < -11$. Copper solubility data define two distinct populations in Cu concentration − log fO_2 space, defined by the composition of the quenched sulfide liquid and in turn fS_2. Copper and S concentrations in the basaltic glass are negatively correlated and also fall into two populations defined by sulfide liquid composition and fS_2.

Both Cu and Fe sulfide liquid/silicate liquid D values span the range of values reported in the literature. The experimental results illustrate that variations in D values correspond to fluctuations in sulfide melt composition and fS_2/fO_2 ratio. For Fe, FeO appears to be the predominant dissolved species, whereas for Cu, $CuO_{0.5}$ and several possible oxy-sulfide complexes may be important. Both Fe and Cu exhibit a departure from the predicted dependency on ½(log fS_2 − log fO_2) using simple oxide-sulfide exchange reactions. However, variations in D values at constant P, T, and fS_2/fO_2 ratios suggest nonideal mixing and deviation from predicted slopes that are related to changes in the ratios of $\gamma_{FeO}/\gamma_{FeS}$ and $\gamma_{CuO_{0.5}}/\gamma_{CuS_{0.5}}$ (or other Cu-bearing species).

Our experiments illustrate that a range of D_{Cu} (sulfide-silicate) values may be applicable for basaltic systems depending primarily on fS_2/fO_2 ratios and help explain the variation in D values computed from natural samples (e.g., Barnes and Maier, 1999). The range in D_{Cu} (sulfide-silicate) values is sufficient to significantly affect results from most numerical models of mantle sulfide melting or metal depletion during sulfide liquation and concentration. Both fO_2 and fS_2 need to be well constrained for successful numerical simulations. In the

case of the crystallization of mafic silicate melts that contain disseminated sulfide blebs, the changes in fS_2/fO_2 ratios that occur during solidification should be considered in evaluating mineralogical zoning in sulfides. For example, in the Duluth Complex in Minnesota, bornite is commonly found along the margins of cubanite-chalcopyrite-rich interstitial sulfides (Ripley and Alawi, 1986). This relationship may be a function of silicate-sulfide equilibria at varying fS_2/fO_2 conditions rather than solely the result of essentially closed system fractional crystallization of individual sulfide blebs as temperature declines.

Experimentally determined mineral/melt partition coefficients also indicate that silicate minerals may host trace amounts of copper (e.g., Bird, 1971; Seward, 1971; Gaetani and Grove, 1997; Hart and Dunn, 1993). Synchrotron X-ray fluorescence microprobe analyses of minerals from the Duluth Complex in Minnesota indicate maximum values of 219 ppm Cu in cumulate olivine and 132 and 212 ppm Cu in interstitial clinopyroxene and biotite, respectively. Results of our experiments indicate that oxide or oxy-sulfide complexing of copper in silicate melts should be expected and that in the absence of significant sulfide, trace quantities of copper will reside in silicate or oxide minerals. It is also clear that the interaction of externally derived sulfur with a mafic magma may result in the further sequestration of copper. Disseminated sulfides such as those present in the Duluth Complex are compatible with reaction between country rock–derived sulfur and copper held as oxide or oxy-sulfide complexes in the magma.

Acknowledgments—Partial support for this work was provided through National Science Foundation grant EAR 9814204 to E. M. Ripley. Constructive reviews by Katharina Lodders and two anonymous *Geochimica et Cosmochimica Acta* reviewers are gratefully acknowledged. Appreciation is expressed to Ms. Ruth Droppo for preparation of the manuscript.

Associate editor: C. Romano

REFERENCES

Barnes S.-J., Maier W. D. The fractionation of Ni, Cu and the noble metals in silicate and sulfide liquids. In *Dynamic Processes in Magmatic Ore Deposits and Their Application to Mineral Exploration* (Keays R. R., Lesher C. M., LightfootP. C., Farrow C. E. G. Geol. Assoc. Can. Short Course Notes **13**, 1999 69–106.

Bird M. L. *Distribution of Trace Elements in Olivines and Pyroxenes—An Experimental Study*. 1971. Ph.D. dissertation, University of Missouri, Rolla.

Cabri L. J. (1973) New data on phase relations in the Cu-Fe-S system. *Econ. Geol.* **68,** 443–454.

Capobianco C. J. and Amelin A. A. (1994) Metal-silicate partitioning of nickel and cobalt: The influence of temperature and oxygen fugacity. *Geochim. Cosmochim. Acta* **58,** 125–140.

Craig J. R. and Kullerud G. (1969) Phase relations in the Fe-Ni-Cu-S system and their application to magmatic ore deposits. *Econ. Geol. Mon.* **4,** 344–358.

Dingwell D. B., O'Neill H. St. C., Ertel W., and Spottel B. (1994) The solubility and oxidation state of nickel in silicate melt at low oxygen fugacities: Results using a mechanically assisted equlibration technique. *Geochim. Cosmochim. Acta* **58,** 1967–1974.

Fleet M. E. and Pan Y. (1994) Fractional crystallization of anhydrous sulfide liquid in the system Fe-Ni-Cu-S, with application to magmatic sulfide deposits. *Geochim. Cosmochim. Acta* **58,** 3369–3377.

Francis R.D. (1990) Sulfide globules in mid-ocean ridge basalts (MORB) and the effect of oxygen abundance in Fe-S-O liquids on the ability of those liquids to partition metals from MORB and komatiitic magmas. *Chem. Geol.* **85,** 199–213.

Gaetani G. A. and Grove T. L. (1997) Partitioning of moderately siderophile elements among olivine, silicate melt, and sulfide melt: Constraints on core formation in the Earth and Mars. *Geochim. Cosmochim. Acta* **61,** 1829–1846.

Ghiorso M. S. and Sack R. O. (1995) Chemical mass transfer in magmatic processes, IV. A revised and internally consistent thermodynamic model for the interpolation and extrapolation of liquid-solid equilibria in magmatic systems at elevated temperatures and pressures. *Contrib. Mineral. Petrol.* **119,** 197–212.

Hart S. R. and Dunn T. (1993) Experimental cpx/melt partitioning of 24 trace elements. *Contrib. Mineral. Petrol.* **113,** 1–8.

Haughton D. R., Roeder P. L., and Skinner B. J. (1974) Solubility of sulfur in mafic magmas. *Econ. Geol.* **69,** 451–467.

Holzheid A. and Lodders K. (2001) Solubility of copper in silicate melts as function of oxygen and sulfur fugacities, temperature, and silicate composition. *Geochim. Cosmochim. Acta* **65,** 1933–1951.

Holzheid A., Borisov A., and Palme H. (1994) The effect of oxygen fugacity and temperature on solubilities of nickel, cobalt, and molybdenum in silicate melts. *Geochim. Cosmochim. Acta* **58,** 1975–1981.

Holzheid A., Palme H., and Chakraboty S. (1997) The activities of NiO, CaO, and FeO in silicate melts. *Chem. Geol.* **139,** 21–38.

Hsieh K.-C., Vlach K. C., and Chang X. A. (1987) The Fe-Ni-S system I. A Thermodynamic analysis of the phase equilibria and calculation of the phase diagram from 1173 to 1623 K. *High Temp. Sci.* **23,** 17–38.

Li C., Naldrett A. J., Coats C. J. C., and Johannessen P. (1992) Platinum, palladium, gold, and copper-rich stringers at the Strathcona mine, Sudbury: Their enrichment by fractionation of a sulfide liquid. *Econ. Geol.* **87,** 1584–1598.

Li C., Barnes S.-J., Makovicky E., Rose-Hansen J., and Makovicky M. (1996) Partitioning of nickel, copper, iridium, rhodium, platinum, and palladium between monosulfide solid solution and sulfide liquid: Effects of composition and temperature. *Geochim. Cosmochim. Acta* **60,** 1231–1238.

Lorand J. P. (1989) Sulfide petrology of spinel and garnet pyroxenite layers from mantle-derived spinel lherzolite massifs of Ariège, northeastern Pyrenees, France. *J. Petrol.* **30,** 987–1015.

Nagamori M., Hatakeyama T., and Kameda M. (1969) Thermodynamics of the iron-sulfur melts in the temperature range of 1100°-1300°C. *J. Jap. Inst. Metals* **33,** 366–370.

Naldrett A. J. (1989) *Magmatic Sulfide Deposits*. Clarendon Press, New York.

Peach C. L. and Mathez E. A. (1993) Sulfide melt-silicate melt distribution coefficients for nickel and iron and implications for the distribution of other chalcophile elements. *Geochim. Cosmochim. Acta* **57,** 3013–3021.

Peach C. L., Mathez E. A., and Keays R. R. (1990) Sulfide melt-silicate melt distribution coefficients for noble metals and other chaldophile elements as deduced from MORB: Implications for partial melting. *Geochim. Cosmochim. Acta* **54,** 3379–3389.

Rajamani V. and Naldrett A. J. (1978) Partitioning of Fe, Co, Ni, and Cu between sulfide liquid and basaltic melts and the composition of Ni-Cu sulfide deposits. *Econ. Geol.* **73,** 82–93.

RipleyE. M.Systematics of sulfur and oxygen isotopes in mafic igneous rocks and related Cu-Ni-PGE mineralization. In *Dynamic Processes in Magmatic Ore Deposits and Their Application to Mineral Exploration* (Keays R. R., Lesher C. M., Lightfoot P. C., Farrow C. E. G. Geol. Assoc. Can. Short Course Notes **13**, 1999 133–158.

Ripley E. M. and Alawi J. (1986) Sulfide mineralogy and chemical evolution of the Babbitt Cu-Ni deposit, Duluth Complex, Minnesota. *Can. Mineral.* **24,** 347–368.

Ripley E. M. and Brophy J. G. (1995) Solubility of copper in a sulfur-free mafic melt. *Geochim. Cosmochim. Acta* **59,** 5027–5030.

Seward T. M. (1971) The distribution of transition elements in the system $CaMgSi_2O_6$-$Na_2Si_2O_5$-H_2O at 1000 bars pressure. *Chem. Geol.* **7,** 73–95.

Vaughan D. J., Burns R. G. Mössbauer spectroscopy and bonding in sulfide minerals containing four-coordinated iron. In: *Proceedings of the 24th International Geology Congress, Montreal*, 1972, pp. 156–167.